Cryogenics xxx (2016) xxx–xxx

Contents lists available at ScienceDirect

Cryogenics

journal homepage: www.elsevier.com/locate/cryogenics

Research paper

Development of a compact cryocooler system for high temperature superconductor filter application

Xiaomin Pang [a,b], Xiaotao Wang [a,*], Jian Zhu [c], Shuai Chen [c], Jianying Hu [a], Wei Dai [a], Haibing Li [c], Ercang Luo [a]

[a] Key Laboratory of Cryogenics, Chinese Academy of Sciences, Beijing 100190, China
[b] Graduate University of Chinese Academy of Sciences, Beijing 100190, China
[c] Lihan Cryogenics Co., Ltd, Shenzhen 518055, China

ARTICLE INFO

Article history:
Received 20 January 2016
Received in revised form 12 May 2016
Accepted 2 June 2016
Available online xxxx

Keywords:
Thermoacoustic theory
Co-axial pulse tube cryocooler
Power density
High frequency

ABSTRACT

Seeking a higher specific power of the pulse tube cryocooler is an important trend in recent studies. High frequency operation (100 Hz and higher), combined with co-axial configuration, serve as a good option to meet this requirement. This paper introduces a high efficiency co-axial pulse tube cryocooler operating at around 100 Hz. The whole system weighs 4.3 kg (not including the radiator) with a nominal input power of 320 W, namely, power density of the system is around 74 W/kg. The envelop dimensions of the cold finger itself is about 84 mm in length and 23 mm in outer diameter. Firstly, numerical model for designing the system and some simulation results are briefly introduced. Distributions of pressure wave, the phase difference between the pressure wave and the volume flow rate and different energy flow are presented for a better understanding of the system. After this, some of the characterizing experimental results are presented. At an optimum working point, the cooling power at 80 K reaches 16 W with an input electric power of 300 W, which leads to an efficiency of 15.5% of Carnot.

© 2016 Elsevier Ltd. All rights reserved.

1. Introduction

Superconductivity has, over the century since its discovery by Kamerlingh Onnes in 1911, found important applications such as generating high magnetic field for scientific research and high sensitivity SQUID device [1]. In 1980s, the discovery of high temperature superconductors (HTS) led to a new boom for superconductivity research. As people are trying to extending the application fields for HTS [2,3], HTS filter is one of the most attractive applications. For this, small-scale and easy-to-be-packaged cryocooler plays an important supporting role. Among several options, Stirling or Stirling type pulse tube cryocooler are good candidates [4,5]. Especially, the pulse tube cryocooler (PTC) is famous for its advantages such as low vibration, high reliability, robustness and low cost due to absence of the moving parts at the cold end. However, existence of a hollow pulse tube and reservoir brings down the system specific power if compared with Stirling cryocooler [6]. A natural choice to make up for this disadvantage is to increase the working frequency [7]. Lots of studies on this have been reported since 2005. In 2007, NIST in America reported a 120 Hz in-line pulse tube cryocooler [8], which could obtain 3.55 W cooling power at 80 K and the relative efficiency of Carnot reached 19.7% based on input acoustic power. NGST developed a high frequency co-axial pulse tube cryocooler in 2009 [9]. The cooling power at 77 K was 1.3 W with 46 W electric power input under 124 Hz operating frequency. The estimated mass of the mechanical cooler in a flight configuration is only 900 g, including the drive electronics. Gan et al. developed a 120 Hz pulse tube cryocooler in 2009 [10]. A cooling power of 8.0 W at 78.5 K as well as a rapid cooling down to 79.8 K in 5 min was achieved.

The research of 100 Hz PTCs at our laboratory has been carried out since 2007. The paper [11] designed an in-line PTC driven by a single piston linear compressor, the no-load temperature reached 59.6 K. In 2009, an in-line PTC combined with a single-piston linear compressor was designed and experimented. A no-load temperature of 31.8 K and a cooling power of 12.5 W at 77 K were obtained with 185.2 W electric power input, the corresponding relative Carnot efficiency of the whole system reached 18.9%, which was the highest efficiency reported at that time [12].

Although the efficiency of the in-line PTC in paper [12] is high, the whole system weighs about 8.9 kg, which is far more than that of a Stirling cryocooler with a similar cooling performance. Meanwhile, in in-line configuration, the cold end heat exchanger is located in the middle of the cryocooler, which is not suitable for practical applications. Therefore, further development is

* Corresponding author.
E-mail address: xtwang@mail.ipc.ac.cn (X. Wang).

http://dx.doi.org/10.1016/j.cryogenics.2016.06.004
0011-2275/© 2016 Elsevier Ltd. All rights reserved.

Please cite this article in press as: Pang X et al. Development of a compact cryocooler system for high temperature superconductor filter application. Cryogenics (2016), http://dx.doi.org/10.1016/j.cryogenics.2016.06.004

needed. This paper introduces an important upgrade of our previous system, which is of co-axial configuration and weighs only 4.6 kg. The compactness and specific power of the system is much improved. In the following sections, the numerical model is firstly presented. Secondly, some simulation results are discussed. Thirdly, the system configuration is briefly introduced and characterizing experimental results are given. Finally, some conclusions are drawn.

2. Numeric method

2.1. Numeric model

The simulation model employed to design the cold head in this paper is based on thermoacoustic theory. According to classic thermoacoustic theory, the momentum, continuity and energy equations are as follows [13,14].

$$dU_1/dx = -\frac{i\omega A}{\gamma p_m}[\xi_c + (\gamma-1)\xi_k f_k]\cdot p_1 + Z\cdot U_1 \quad (1)$$

$$dp_1/dx = -(i\omega\xi_l l + \xi_v r_v)U_1 \quad (2)$$

$$dH/dx = -Q \quad (3)$$

where p_1, U_1 are the pressure and volume flow rate, respectively. ω is the angular frequency. p_m is the mean pressure. f_k is related to the configuration and dimensions of the flow channel. Z is acoustic impendence which is a function of the temperature gradient. r_v, l represent the viscous resistance and inertance, respectively. H is the total energy flow. Q is the heat transfer between each component and the surroundings. Considering the turbulent flow in practical pulse tube cryocooler, four correction factors $\xi_c, \xi_k, \xi_l, \xi_v$ are introduced in Eqs. (1) and (2). Details of these formulations can be found in [13–15]. The calculation algorithm can be found in Ref. [16].

The governing equations for linear compressor are

$$\hat{E} - BL\hat{u} = \hat{I}(R_e + i\omega L_e) \quad (4)$$

$$\hat{I}BL = \hat{p}A + k\frac{\hat{u}}{i\omega} + R_m\hat{u} + mi\omega\hat{u} \quad (5)$$

where $\hat{E}$ is applied electric voltage, BL is force factor, $\hat{u}$ is the piston velocity, R_e and L_e are resistance and inductance of the motor coil, respectively. $\hat{p}$ is the pressure wave at the piston front side. k is spring constant. R_m is the damping coefficient. Details of the calculation algorithm of matching compressor and cold head can be found in Ref. [17].

2.2. General procedures in design

Firstly, systematical calculations have been done to optimize the dimensions of the 100 Hz co-axial cold head with the thermal efficiency as the primary target. Considering the possible discrepancy between simulation and experiments from previous experiences, some margins on both efficiency and cooling power are kept. Final dimensions of the cold head, listed in Table 1, are determined with some practical considerations due to the co-axial configuration.

Once the cold head design is determined, based on the cold head acoustic impedance and the compressor mechanical governing equations, i.e. Eqs. (4) and (5), parameters of the linear compressor are calculated and determined as shown in Table 2.

Table 1
Main parameters of the pulse tube cryocooler.

Components	Diameter (mm)	Length (mm)
Main ambient exchanger	i.d. 20	30
Regenerator	Outside diameter, 22.5 Inside diameter, 10.4	35
Cold end heat exchanger	i.d. 20	8.4
Pulse tube	10	54
Secondary ambient heat exchanger	10	5
Inertance tube	3	1500
Reservoir	130 cm^3	

Table 2
Details of the compressor parameters.

BL (N/A)	R_e (Ω)	R_m (N s/m)	M (kg)	D (mm)	L_e (mH)	K (kN/m)	Void volume of the front chamber (cm^3)
16	0.43	14	0.32	22	0.2	62.7	7

3. Simulation results

The geometric model is presented in Fig. 1. Temperatures of the ambient heat exchanger and the cold end heat exchanger are set at 308 K and 80 K, respectively. The mean pressure is set to be 3.5 MPa with helium and the operating frequency is set at 100 Hz. For the regenerator, 600-mesh stainless steel screens with a wire diameter of 18 μm are used.

According to the numerical model introduced in last section, the optimized performance is obtained with 300 W input electric power, and the optimized relative Carnot efficiency of the whole system is about 17.4%. In order to further understand the

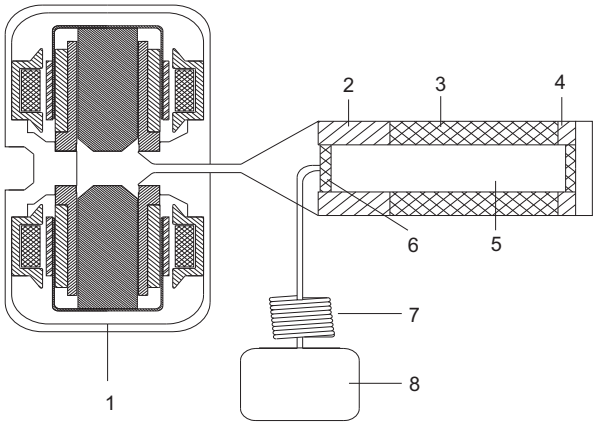

1.compressor 2.main ambient heat exchanger 3.regenerator 4.cold end heat exchanger 5.pulse tube 6.secondary ambient heat exchanger 7.inertance tube 8.reservoir

Fig. 1. Schematic of a 100 Hz co-axial pulse tube cryocooler.

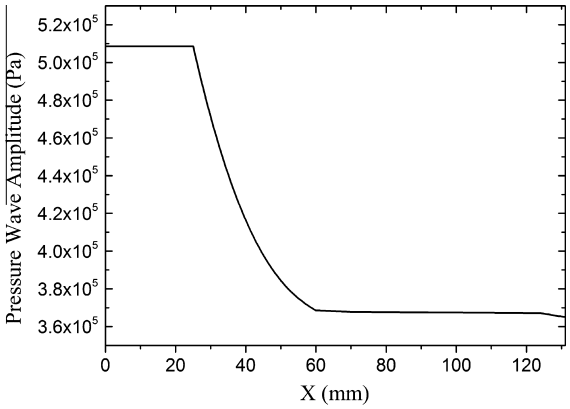

Fig. 2. Axial distribution of pressure wave amplitude.

Please cite this article in press as: Pang X et al. Development of a compact cryocooler system for high temperature superconductor filter application. Cryogenics (2016), http://dx.doi.org/10.1016/j.cryogenics.2016.06.004

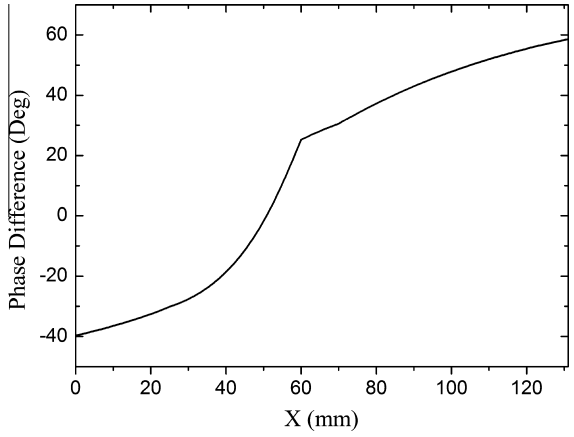

Fig. 3. Axial distribution of phase difference between pressure wave and volume flow rate.

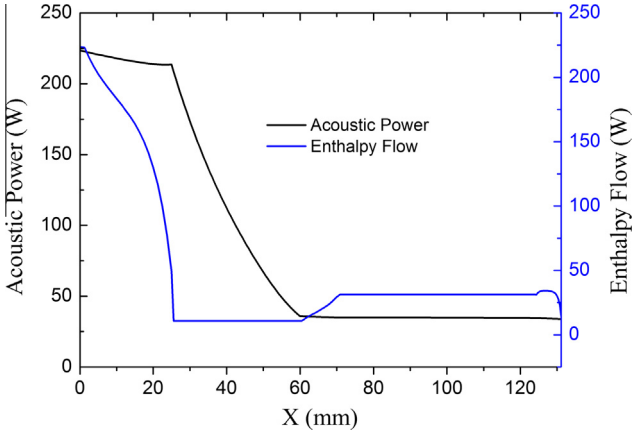

Fig. 4. Axial distribution of acoustic work and enthalpy flow.

performance of the PTC system, the axial distributions of some important parameters at this operating point are presented in Figs. 2–4. The x coordinate begins at the main ambient heat exchanger and goes to the regenerator, the cold end heat exchanger, the pulse tube and the secondary ambient heat exchanger.

Fig. 2 shows the axial distribution of the pressure wave amplitude. It indicates that the pressure drop is primarily due to the regenerator. In the heat exchanger and the pulse tube, the pressure drop is small. As seen in Fig. 3, the phase difference between pressure wave and volume flow rate inside the regenerator varies from −30° to 25.5°, indicating an in-phase relationship between the pressure wave and volume flow rate has been obtained inside the regenerator. This is significant for obtaining a high efficiency. At the outlet of the secondary ambient heat exchanger, the pressure wave leads the volume flow rate by about 60°, which is a typical phase angle generated by the inertance tube plus reservoir. Fig. 4 shows that most acoustic power is consumed in the regenerator. About 30 W acoustic power is dissipated in the inertance tube and reservoir. The distribution of enthalpy flow is also given in Fig. 4. About 18.6 W cooling power is obtained at the cold end.

4. Experiments

4.1. Experimental setup

Based on the numerical simulations, a co-axial PTC system has been developed in reference to Tables 1 and 2. Fig. 5 is a photo of

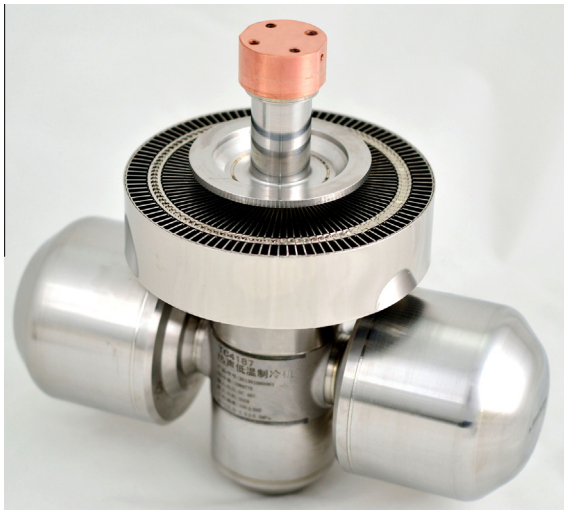

Fig. 5. Photo of the cryocooler system.

the cryocooler. The whole system weighs 4.3 kg (not including the radiator), much smaller than that of the in-line PTC in Ref. [12]. A maximum input electrical power of the system can reach 320 W, i.e. a power density of 74 W/kg, which is similar to that of a typical CryoTel™ CT developed by Sunpower [18].

The PTC system uses air cooling. For obtaining a more compact structure, the reservoir of the phase shifter is located between the dual-opposed motor and the inertance tube is located inside the reservoir. The envelop dimensions of the cold finger itself is about 84 mm in length and 23 mm in outer diameter.

The linear compressor is of moving-magnet type. Dual-opposed motor configuration is used to ensure an easy cancellation of vibration. Gas-bearing technology is applied in the compressor to ensure the small clearance between the piston and cylinder and it is easier to realize a bigger specific power as compared with flexure bearing technology.

The mean pressure of the system is 3.5 MPa. The operating frequency is set to 100 Hz, if not specially mentioned. A platinum resistance thermometer with an accuracy of ±0.1 K is attached to the cold end heat exchanger to measure the temperature. Cooling power is measured through a heating wire which is mounted on the cold end heat exchanger powered by a DC voltage source.

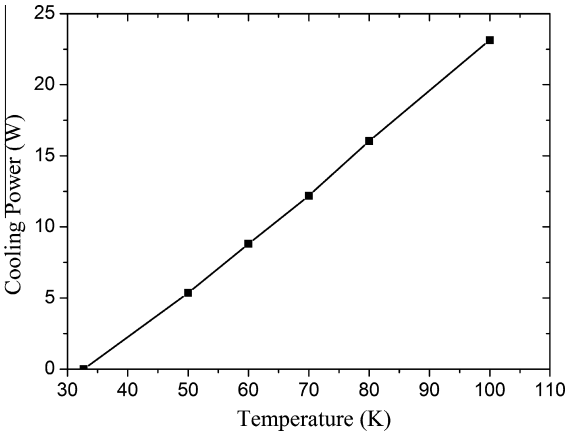

Fig. 6. 80 K Cooling power vs. temperature of the cold end heat exchanger, the electrical power input is kept at 300 W.

Please cite this article in press as: Pang X et al. Development of a compact cryocooler system for high temperature superconductor filter application. Cryogenics (2016), http://dx.doi.org/10.1016/j.cryogenics.2016.06.004

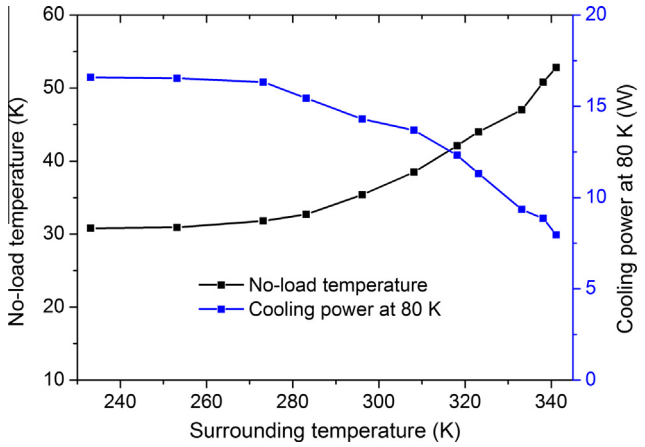

Fig. 7. No-load temperature and cooling power at 80 K vs. surrounding temperature the electrical power input is kept at 300 W.

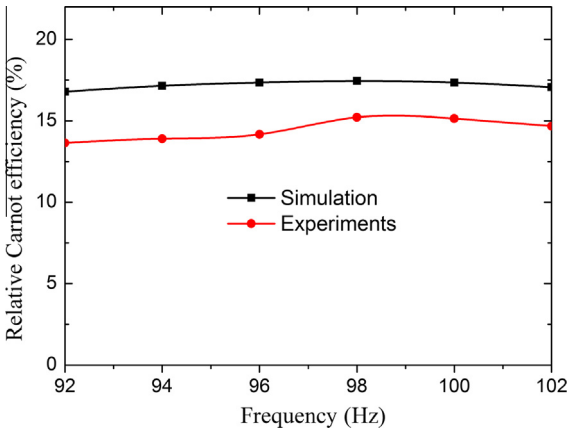

Fig. 8. Relative Carnot efficiency of the whole system vs. frequency, with 10 W cooling power at 80 K.

4.2. Characterizing experimental results and discussions

Fig. 6 depicts the relationship between the cold head temperature and the cooling power with a given input electric power. The cooling power is 5.35 W at 50 K with a reject temperature of 308 K, corresponding to a relative Carnot efficiency of 9%. When the cold head temperature rises to 80 K, the cooling power is increased to 16 W and the relative Carnot efficiency reaches 15.5%.

In order to investigate the adaptability of the cryocooler to various environments, influence of the surrounding temperature is studied. The experiments are done in a thermostat, and Fig. 7 shows the experimental results with a given electrical power. With decreasing surrounding temperature from 340 K to around 270 K, the lowest no-load temperature decreases and the cooling power at 80 K increases. Then the performance becomes less sensitive to the surrounding temperature below 270 K.

The surrounding temperature affects the heat rejection temperature, which influence the performance of the PTC system. With decreasing the heat rejection temperature, the efficiency of the cold head normally increases. Cooling power will increase with the same input acoustic power. However, the whole system is a resonant system and the surrounding temperature also affects the mean pressure. With the surrounding temperature decreasing, the mean pressure reduces monotonically and the dynamic behavior of the system also changes, which include the resonance frequency of the linear compressor, the match between the compressor and the cold head and the impedance of the inertance tube. Thus the efficiency of compressor is inevitably influenced as well as the cold head. Tendency shown in Fig. 7 are due to these combined effects, which needs further investigation.

The influence of operating frequency on the system performance is also investigated. Fig. 8 shows the dependence of relative Carnot efficiency of the whole system on frequency. The cooling power is kept 10 W at 80 K through adjusting the input electric power of the compressor. In the experiments, the system has an optimal performance around 98 Hz. The corresponding input electric power is 191 W and the relative Carnot efficiency is 15.2%. At 100 Hz, the relative Carnot efficiency slightly decreases to 15.1%.

4.3. A comparison with simulation

Fig. 8 compares the relative Carnot efficiency of the whole system with different frequency between experiments and simulations. The cooling performance from the simulation is better than that from the experiments under the same operating conditions. This may arise from the quasi-one-dimensional simplification of the numerical model. Complicated losses, such as the loss due to flow reversal happening at the cold end heat exchanger, are not considered here. The model will be further improved through CFD simulation of some key components as well as using some correction factors based on lots of systematical experiments.

5. Conclusions

A high efficiency and high specific power pulse tube cryocooler system which combines high frequency operation (100 Hz) with co-axial configuration has been introduced in this paper.

Based on thermoacoustic theory and governing equations for linear compressor, numerical simulation is performed to design and optimize the PTC system. Simulation results indicate that a cooling power of 18.6 W at 80 K and a relative Carnot efficiency of 17.4% can be achieved with 3.5 MPa helium and 100 Hz operating frequency. Axial distributions of some important parameters are studied to better understand the performance of the system.

A co-axial PTC system has been developed based on the simulation results. The envelop dimensions of the cold finger itself is about 84 mm in length and 23 mm in outer diameter. The whole system weighs 4.3 kg and the electric power density reaches 74 W/kg. With an input electrical power of 300 W, 16 W cooling power at 80 K can be obtained, which leads to a relative Carnot efficiency of 15.5%. Improving the numerical model to reduce the discrepancy between the simulations and experiments is our future work.

Acknowledgements

The authors would like to thank Zhongke Lihan Inc. for their technical support. This work is financially supported by the National Natural Science Foundation of China (Contract number 51206177, 51576205) and National High Technology Research and Development Program of China (Contract number 2014AA032703).

References

[1] Nishijima S, Eckroad S, Marian A, et al. Superconductivity and the environment: a roadmap. Supercond Sci Technol 2013;26(11):113001.
[2] Kuriyama T, Urata M, Yazawa T, et al. Cryocooler directly cooled 6 T NbTi superconducting magnet system with 180 mmroom temperature bore. Cryogenics 1994;34(Suppl. 1):643–6.
[3] Noe M, Steurer M. High-temperature superconductor fault current limiters: concepts, applications, and development status. Supercond Sci Technol 2007;20(3):R15.
[4] Radebaugh R. Development of the pulse tube refrigerator as an efficient and reliable cryocooler. In: Proc Institute of Refrigeration (London).

[5] Radebaugh R. The development and application of cryocoolers since 1985. In: Proceedings of ICCR'2003. International Academic Publishers/Beijing World Publishing Corporation; 2003. p. 858–70.
[6] Radebaugh R. Pulse tube cryocoolers for cooling infrared sensors. In: International symposium on optical science and technology. International Society for Optics and Photonics; 2000. p. 363–79.
[7] Radebaugh Ray, Garaway Isaac, Veprik Alexander M. Development of miniature, high frequency pulse tube cryocoolers. International Society for Optics and Photonics; 2010. p. 76602J-76602J-14.
[8] Vanapalli S, Lewis M, Gan Z, et al. 120 Hz pulse tube cryocooler for fast cooldown to 50 K. Appl Phys Lett 2007;90. 072504:1-3.
[9] Petach M, Waterman M, Pruitt G, Tward E. High frequency coaxial pulse tube microcooler. Cryocoolers 2008;15:97–103.
[10] Wu YZ, Gan ZH, Qiu LM, et al. Study on a single-stage 120 Hz pulse tube cryocooler. AIP Conf Proc 2010;1218(1):175.
[11] Wang X, Dai W, Luo EC, et al. Characterization of a 100 Hz miniature pulse tube cooler driven by a linear compressor. Adv in cryogenic engineering, vol. 55A. Melville (NY): Amer. Institute of Physics; 2010. p. 183–90.
[12] Wang XT, Dai W, Hu JY, et al. Performance of a Stirling-type pulse tube cooler for high efficiency operation at 100 Hz. Cryocooler 2011;16.
[13] Swift GW. Thermoacoustics: a unifying perspective for some engines and refrigerators. New York: AIP Press; 2002.
[14] Xiao JH. Thermoacoustic heat transportation and energy transformation Part 1: Formulation of the problem. Cryogenics 1995;35:15–9.
[15] Ward WC, Swift GW. Design environment for low-amplitude thermoacoustic engines [43.35.Ud, 43.20.Mv]. J Acoust Soc Am 1994;95(6):3671–2.
[16] Dai W, Luo EC, Zhang Y, et al. Detailed study of a traveling wave thermoacoustic refrigerator driven by a traveling wave thermoacoustic engine. J Acoust Soc Am 2006;119(5):2686–92.
[17] Dai Wei, Luo Ercang, Wang Xiaotao, Wu Zhanghua. Impedance match for Stirling type cryocoolers. Cryogenics 2011;51:168–72.
[18] Unger R, Keiter D. The development of the CryoTel™ family of coolers. In: Adv Cryog Eng: Trans. p. 1404–11.

Please cite this article in press as: Pang X et al. Development of a compact cryocooler system for high temperature superconductor filter application. Cryogenics (2016), http://dx.doi.org/10.1016/j.cryogenics.2016.06.004